Mid-IR imaging of the transitional disk of HD169142: Measuring the size of the gap
— Source link ⎋

Mitsuhiko Honda, K. M. Maaskant, Yoshizo Okamoto, Hirokazu Kataza ...+13 more authors

Related papers:

- Mid-infrared Imaging of the Transitional Disk of HD 169142: Measuring the Size of the Gap

- Identifying gaps in flaring Herbig Ae/Be disks using spatially resolved mid-infrared imaging - Are all group I disks transitional?

- ISO spectroscopy of circumstellar dust in 14 Herbig Ae/Be systems: Towards an understanding of dust processing

- Gaps in the HD169142 protoplanetary disk revealed by polarimetric imaging: Signs of ongoing planet formation?

- Gaps in the hd 169142 protoplanetary disk revealed by polarimetric imaging: signs of ongoing planet formation?

Share this paper: 📘 🐦 in ✉

View more about this paper here: https://typeset.io/papers/mid-ir-imaging-of-the-transitional-disk-of-hd169142-rq8lf0wek5

MID-INFRARED IMAGING OF THE TRANSITIONAL DISK OF HD 169142: MEASURING THE SIZE OF THE GAP[*]

M. HONDA[1], KOEN MAASKANT[2,3], Y. K. OKAMOTO[4], H. KATAZA[5], M. FUKAGAWA[6], L. B. F. M. WATERS[2,7],
C. DOMINIK[2,8], A. G. G. M. TIELENS[3], G. D. MULDERS[2,9], M. MIN[10], T. YAMASHITA[11], T. FUJIYOSHI[12],
T. MIYATA[13], S. SAKO[13], I. SAKON[14], H. FUJIWARA[12], AND T. ONAKA[14]

[1] Department of Mathematics and Physics, Faculty of Science, Kanagawa University, 2946 Tsuchiya, Hiratsuka, Kanagawa 259-1293, Japan
[2] Astronomical Institute Anton Pannekoek, University of Amsterdam, P.O. Box 94249, 1090 GE Amsterdam, The Netherlands
[3] Leiden Observatory, Leiden University, P.O. Box 9513, 2300 RA Leiden, The Netherlands
[4] Institute of Astrophysics and Planetary Sciences, Faculty of Science, Ibaraki University, 2-1-1 Bunkyo, Mito, Ibaraki 310-8512, Japan
[5] Department of Infrared Astrophysics, Institute of Space and Astronautical Science, Japan Aerospace Exploration Agency,
3-1-1 Yoshinodai, Sagamihara, Kanagawa 229-8510, Japan
[6] Department of Earth and Space Science, Graduate School of Science, Osaka University, 1-1 Machikaneyama, Toyonaka, Osaka 560-0043, Japan
[7] SRON Netherlands Institute for Space Research, Sorbonnelaan 2, 3584 CA Utrecht, The Netherlands
[8] Department of Astrophysics/IMAPP, Radboud University Nijmegen, P.O. Box 9010, 6500 GL Nijmegen, The Netherlands
[9] SRON Netherlands Institute for Space Research, P.O. Box 800, 9700 AV Groningen, The Netherlands
[10] Astronomical Institute Utrecht, Utrecht University, P.O. Box 80000, 3508 TA Utrecht, The Netherlands
[11] National Astronomical Observatory of Japan, 2-21-1 Osawa, Mitaka, Tokyo 181-8588, Japan
[12] Subaru Telescope, National Astronomical Observatory of Japan, 650 North A'ohoku Place, Hilo, HI 96720, USA
[13] Institute of Astronomy, School of Science, University of Tokyo, 2-21-1 Osawa, Mitaka, Tokyo 181-0015, Japan
[14] Department of Astronomy, Graduate School of Science, University of Tokyo, Bunkyo-ku, Tokyo 113-0033, Japan

ABSTRACT

The disk around the Herbig Ae star HD 169142 was imaged and resolved at 18.8 and 24.5 μm using Subaru/COMICS. We interpret the observations using a two-dimensional radiative transfer model and find evidence for the presence of a large gap. The mid-infrared images trace dust that is emitted at the onset of a strong rise in the spectral energy distribution (SED) at 20 μm, and are therefore very sensitive to the location and characteristics of the inner wall of the outer disk and its dust. We determine the location of the wall to be 23^{+3}_{-5} AU from the star. An extra component of hot dust must exist close to the star. We find that a hydrostatic optically thick inner disk does not produce enough flux in the near-infrared, and an optically thin, geometrically thick component is our solution to fit the SED. Considering the recent findings of gaps and holes in a number of Herbig Ae/Be group I disks, we suggest that such disk structures may be common in group I sources. Classification as group I should be considered a strong case for classification as a transitional disk, though improved imaging surveys are needed to support this speculation.

Key words: circumstellar matter – protoplanetary disks – stars: pre-main sequence

1. INTRODUCTION

Transitional disks are a class of protoplanetary disks whose inner regions are devoid of small dust grains. These disks have been attracting attention recently, since such cleared inner regions or gaps may be related to ongoing planet formation. The presence of an inner hole/gap has been suggested for the disk around the Herbig Ae star HD 169142 by Grady et al. (2007) and Meeus et al. (2010), mostly based on analysis of the spectral energy distribution (SED). Both groups conclude that the steep rise in flux at ∼20 μm in the SED reflects emission from the wall of the outer disk. The location of the wall (i.e., the inner edge of the outer disk) has not been determined conclusively—Meeus et al. (2010) used 20 AU while Grady et al. (2007) suggested 44 AU. Observations of HD 169142 at various wavelengths have so far not been able to constrain the inner cavity radius directly and accurately.

One of the limitations of SED modeling is the inability to locate and prove the existence of gaps in protoplanetary disks. For instance, gaps may not be revealed in the SED because the inner disk can partially obscure large parts of the outer disk (Acke et al. 2009) and gaps hidden under that shadow do not leave a fingerprint in the SED. Clever SED modeling can reproduce SEDs of truly transitional disks without the need for a gap. The transitional disk LkCa 15 has an outer disk starting at 46 AU as seen at 1.4 and 2.8 mm wavelengths (Piétu et al. 2006). However, Isella et al. (2009) show that a model approach with a smooth distribution of material from a few stellar radii to about 240 AU can sometimes reproduce both the observed SED and the spatially resolved continuum emission at millimeter wavelengths for this object. Only from direct imaging is it possible to directly constrain the radial density structure of dust in a protoplanetary disk.

Dust in protoplanetary disks covers a temperature range from ∼1500 K at the inner dust sublimation radius to a few Kelvin in the outer parts of the disk. Direct mid-infrared (MIR) imaging at 18.8 and 24.5 μm is most sensitive for 100–150 K blackbody dust, though strong contributions from dust elsewhere in the disk at lower and higher temperatures can also be present. If the disk has a very strong near-infrared (NIR) component such as HD 135344 (Meeus et al. 2001), the inner region may still be strongly represented in the center of the image at 18 μm. On the other hand, for disks with a larger gap or an inner hole, the image size will be a sensitive tracer for the location of the inner radius of the outer disk (Verhoeff et al. 2011).

In this paper, we present direct MIR imaging observations of HD 169142 at 18.8 and 24.5 μm, using the Cooled

Table 1
Summary of Observations

Object	Filter	Date (UT)	Integ. Time (s) Used/Total (%)	Airmass	Direct FWHM
δOph	Q24.5	2004 Jul 11	195/243 s (80%)	1.254–1.354	$0\rlap{.}''628 \pm 0\rlap{.}''007$
HD 169142	Q24.5	2004 Jul 11	345/802 s (43%)	1.541–1.542	$0\rlap{.}''680 \pm 0\rlap{.}''034$
αHer	Q18.8	2004 Jul 12	83/83 s (100%)	1.081–1.115	$0\rlap{.}''493 \pm 0\rlap{.}''006$
HD 169142	Q18.8	2004 Jul 12	215/360 s (60%)	1.553–1.559	$0\rlap{.}''604 \pm 0\rlap{.}''017$

Mid-Infrared Camera and Spectrometer (COMICS) on the 8.2 m Subaru telescope. We confirm the result found by Mariñas et al. (2011) and find that the disk shows extended emission at 18 μm. In addition we find that the disk is also resolved at 24.5 μm. By constructing a radiative transfer disk model that fits both the SED and the imaging results, we find that the size of the source at MIR wavelengths is most naturally explained by a disk with a large inner gap, i.e., a transitional disk. We discuss the structure of the disk and the implications for its nature.

2. OBSERVATIONS AND DATA REDUCTION

Observations were conducted using COMICS (Kataza et al. 2000; Okamoto et al. 2003; Sako et al. 2003) on the 8.2 m Subaru Telescope on Mauna Kea, Hawaii. HD 169142 was observed using the Q24.5-NEW ($\lambda = 24.5$ μm, $\Delta\lambda = 0.75$ μm) and Q18.8 ($\lambda = 18.8$ μm, $\Delta\lambda = 0.9$ μm) filters. The plate scale of the COMICS camera was 0.13 arcsec pixel^{-1}. The chopping throw was 10 arcsec and the position angle of the chopping direction was 0°. The chopping frequency was 0.45 Hz. The total integration times for Q24.5 and Q18.8 observations were 802 s and 360 s, respectively. Just before and after observing HD 169142, we took data from point spread function (PSF) reference and photometric standard stars. We used δ Oph for Q24.5 and α Her for Q18.8. The total integration times for the reference stars were 243 s and 83 s, respectively. A summary of the observations is given in Table 1.

We processed the data using a shift-and-add method to improve the blurring caused by atmosphere, tracking errors, misregistration, etc. The imaging data consisted of 0.98 s on-source integration frames. First, the thermal background and the dark current signals were removed through the subtraction of the chopped pair frames. The object and the PSF star are bright enough to be recognized even in 0.98 s chop-subtracted frames, so we searched the centroid of the object. We then shifted the frames so as to align the centroid position and summed up the frames. However, we excluded frames which were blurred by atmospheric seeing. We also rejected frames whose radius of 78.4% encircled energy ($r_{78.4}$) was larger than the threshold radius (r_c) which covers 95% of the wavefronts whose Strehl ratio is 0.9. These threshold values are determined as $r_c = 1\rlap{.}''131$ at 18.8 μm and $r_c = 1\rlap{.}''482$ at 24.5 μm by Monte Carlo simulation of the ideal unresolved point source. Due to this rejection of lower quality data, the effective integration time of HD 169142 was reduced to 345 s and 215 s for Q24.5 and Q18.8, respectively. The same procedure was applied to the PSF images taken before and after HD 169142, where the effective integration time became 195 s and 83 s, respectively. Since HD 169142 shows marginal extension compared to the PSF, and the rejection criterion r_c is determined for the ideal unresolved point source, frame rejection rates of HD 169142 are higher than those of PSF stars. This means that the effective rejection criterion is slightly more stringent for HD 169142 than

for PSF stars, however, it does not overestimate the extension of HD 169142.

For flux calibration we used template spectra provided by Engelke et al. (2006). Using the standard stars observed over the two nights, an airmass correction was applied for Q24.5 photometry. For Q18.8 photometry, we could not find a significant airmass dependence during the night. A standard aperture photometry was applied and the resultant flux density of HD 169142 was 10.5 ± 0.4 Jy at 18.8 μm and 13.0 ± 0.5 Jy at 24.5 μm. The final images of the HD 169142 and PSF stars are shown in Figure 1.

3. RESULTS

3.1. Source Size of HD 169142 at 18.8 and 24.5 μm

The azimuthally averaged radial brightness profiles of HD 169142 and the PSF stars at 18.8 and 24.5 μm are shown in Figure 2. It is clear that HD 169142 is extended at these wavelengths. At 18.8 μm the direct FWHM of the shift-and-added images of HD 169142 and of the PSF stars were $0\rlap{.}''604 \pm 0\rlap{.}''017$ and $0\rlap{.}''493 \pm 0\rlap{.}''006$, respectively. At 24.5 μm, the corresponding numbers are $0\rlap{.}''680 \pm 0\rlap{.}''034$ and $0\rlap{.}''628 \pm 0\rlap{.}''007$ (see Table 1). It is surprising that the size of HD 169142 does not increase with wavelength. For a continuous flaring disk, one would expect the size of the image to scale roughly with the PSF (Meijer 2007). Our images therefore give a first indication that the radial density structure is not continuous. The FWHMs of the PSF references are comparable to the predicted value of the diffraction-limited performance of the telescope. As a rough estimate of the intrinsic source size of HD 169142, we applied the quadratic subtraction method as described by Mariñas et al. (2011). The derived source FWHMs were $0\rlap{.}''349 \pm 0\rlap{.}''014$ at 18.8 μm and $0\rlap{.}''261 \pm 0\rlap{.}''025$ at 24.5 μm. Since Mariñas et al. (2011) observed the FWHM of this source to be $0\rlap{.}''32 \pm 0\rlap{.}''05$ at 18.0 μm, our measurement at 18.8 μm is in good agreement with their results within the uncertainties.

4. MODELING

4.1. Observational Constraints

Complementary views of the disk structure and the dust properties of HD 169142 are obtained by adopting photometric data at various wavelengths from the literature (van den Ancker et al. 1997; Cutri et al. 2003; Zacharias et al. 2004; Sylvester et al. 1996; Meeus et al. 2010) and MIR spectra from *ISO* (Meeus et al. 2001) and *Spitzer*/Infrared Spectrograph (IRS; Juhász et al. 2010). These data sets reflect the disk brightness as a function of wavelength, and are a result of the disk structure defined by the density distribution, composition, inclination, and inner and outer radius of the disk, and by the properties of the central star. An outer disk radius of 235 AU is taken from Panić et al. (2008). An inner disk radius of 0.1 AU is set at the location where the dust reaches 1500 K and starts to sublimate. With
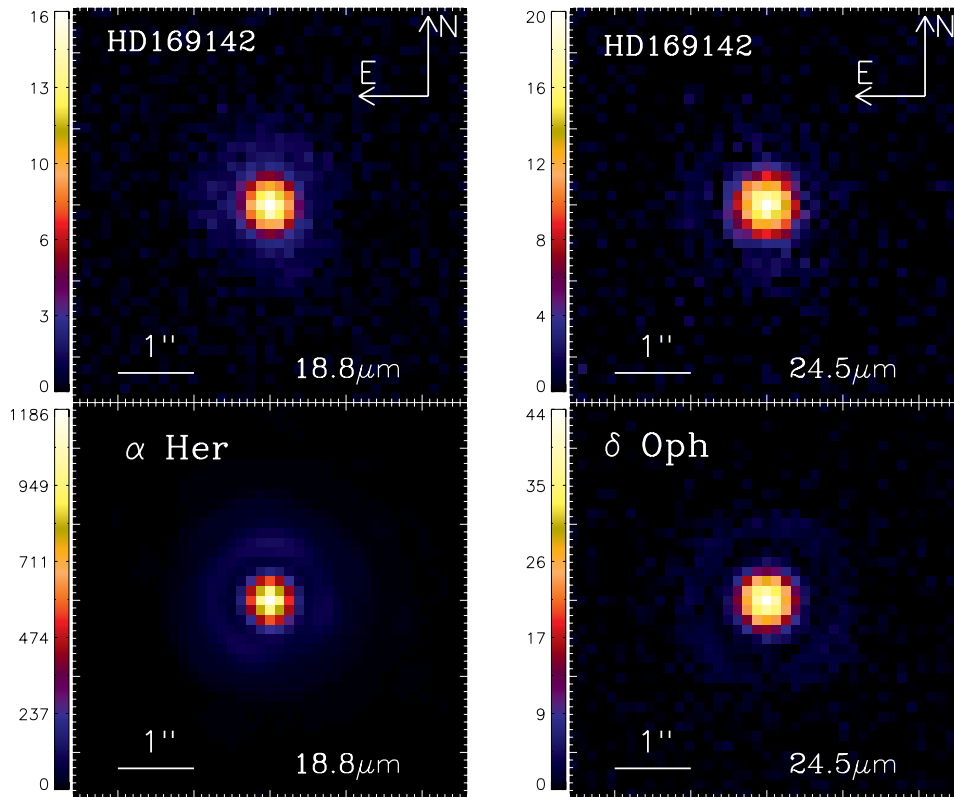
Figure 1. Shift-and-added image of HD 169142 (top) and the PSF stars (bottom) at 18.8 and 24.5 μm. The brightness unit is Jy arcsec^{-2} and is scaled from 0 to the peak value in the image. North is up and east is to the left.
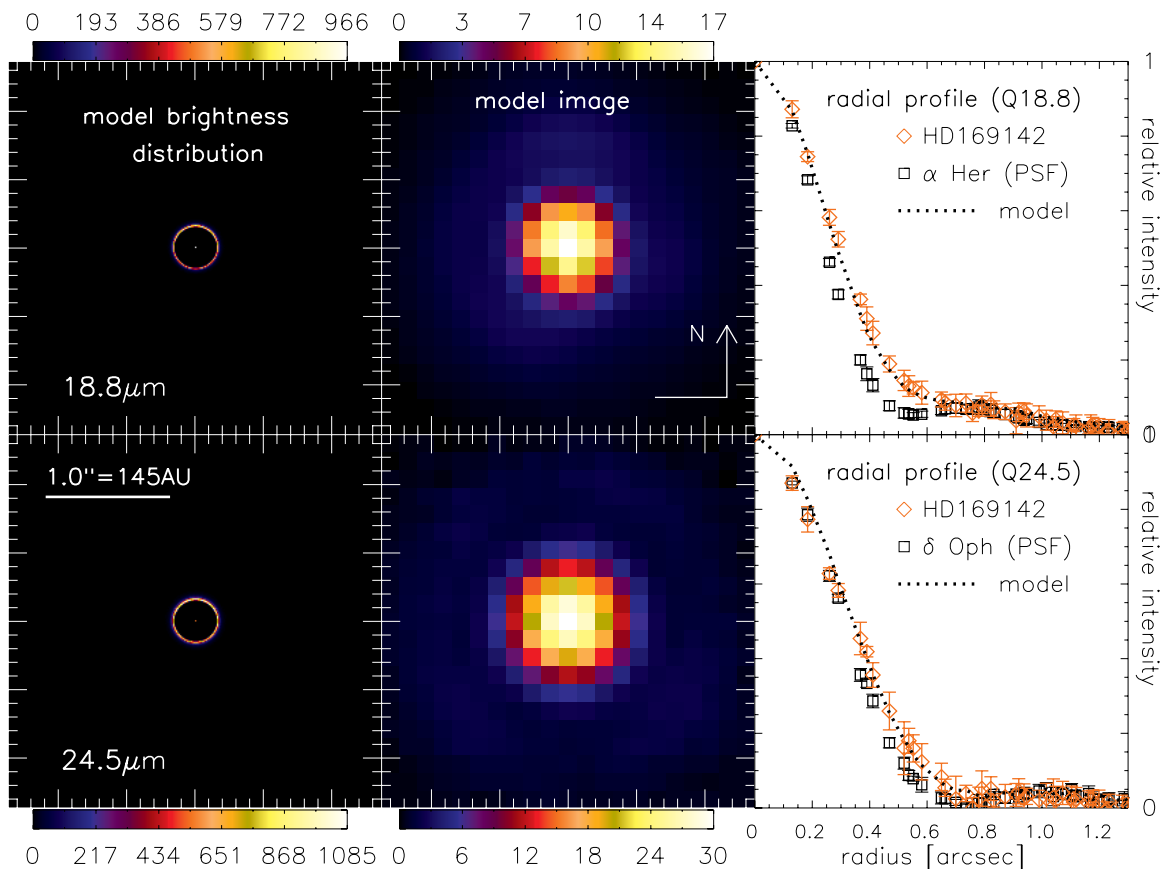

Figure 2. The left and middle panels show the model brightness distribution of the final model and model image after convolving by Subaru/COMICS PSF (middle), respectively, shown in Jy arcsec^{-2}. The right panels represent the peak-normalized azimuthally averaged radial brightness profiles relative to the centroid of the image (right). The top panels are in the Q18.8 and the bottom panels are in the Q24.5 filters. In the radial profile plots (right), the observation of HD 169142 is shown by the red diamonds, and the corresponding PSF of the calibrators is shown by the black squares. The final model convolved with the PSF is shown by the black dotted line.

Table 2
Parameters of HD 169142 System Used in our Best-fit Model

Parameter	Value	Remarks
Spectral type	A5Ve	Dunkin et al. (1997)
Extinction A_V	0.46 ± 0.05	van den Ancker (1999)
log g	4.22	van den Ancker (1999)
Temperature	8200 K	Dunkin et al. (1997)
Distance	145 ± 15 pc	de Zeeuw et al. (1999)
Age	6^{+6}_{-3} Myr	Grady et al. (2007)
Stellar luminosity	$15.33 \pm 2.17\ L_\odot$	van den Ancker (1999)
Stellar mass	$2.28 \pm 0.23\ M_\odot$	van den Ancker (1999)
Stellar radius	$1.94 \pm 0.14\ R_\odot$	van den Ancker (1999)
Gas disk mass	$(0.16\text{–}3.0) \times 10^{-2}\ M_\odot$	Panić et al. (2008)
Dust disk mass	$4 \times 10^{-4}\ M_\odot$	Fit to the submillimeter photometry
Inclination	13°	Raman et al. (2006); Dent et al. (2005)
Accretion rate	$\leqslant 10^{-9}\ M_\odot$ yr^{-1}	Grady et al. (2007)
R_{halo}	0.1–0.2 AU	Geometrically high, optically thin component to fit the NIR
R_{in}	23^{+3}_{-5} AU	Fit to RBP of Subaru/COMICS data
R_{out}	235 AU	Panić et al. (2008)
Surface density exponent	-1.0	Hydrostatic equilibrium
Particle size	$a = \{0.03\,\mu\text{m}, 1\text{ cm}\}$	Power-law distribution of -3.5
Silicates	70%	Similar to Mulders et al. (2011)
Amorphous carbon	30%	Zubko et al. (1996)
M_{PAH}	$0.45 \times 10^{-7}\ M_\odot$	Uniform PAH distribution
M_{halo}	$0.28 \times 10^{-10}\ M_\odot$	Only carbon
M_{disk}	$0.3 \times 10^{-3}\ M_\odot$	Mass of grains $a = \{0.03\,\mu\text{m}, 1\text{ cm}\}$ in the disk

an inclination of 13° (Raman et al. 2006), the system is nearly pole-on and, therefore, deviations from axial symmetry caused by projection effects can be neglected in our images. The stellar spectrum is described by a Kurucz model with an effective temperature of 8200 K (Dunkin et al. 1997), luminosity of $15.3\ L_\odot$ and extinction $A_V = 0.46$ (van den Ancker 1999). The system is set at a distance of 145 pc (de Zeeuw et al. 1999). All stellar and disk parameters used in this paper are shown in Table 2.

4.2. Radiative Transfer Code MCMax

We construct a geometrical model of the disk of HD 169142 and fit it to both the radial surface brightness profile (RBP) of our observed images and to the SED. For the model we use the radiative transfer code MCMax (Min et al. 2009), which is able to solve temperature and density structures in very optically thick circumstellar disks. This code has been compared to other radiative transfer codes by Pinte et al. (2009) and has been applied successfully in previous studies (e.g., Verhoeff et al. 2011; Mulders et al. 2011). We assume an axisymmetric dust distribution in which the optical properties of the grains are computed using a distribution of hollow spheres (Min et al. 2005). We consider all dust species in the disk to be in thermal contact, and calculate their respective opacities from the optical constants as if they were separate particles. Furthermore, we assume the gas temperature to be set by the dust temperature. We adopted grains with sizes according to the power law $f(a) \propto a^{-3.5}$. The power-law index is that of interstellar grains (Mathis et al. 1977) and is consistent with collisional fragmentation considerations (Hellyer 1970). Under the assumption that the system is in hydrostatic equilibrium, the vertical density distribution of the disk is solved by iterating the density and temperature structures until they become self-consistent (e.g., Dullemond et al. 2007).

We assume a grain population consisting of 30% carbon and 70% silicates (we refer to Mulders et al. 2011 for references of the optical properties of this dust composition). The contribution of warm small ($<10\,\mu$m) amorphous silicate grains to the

spectrum must be low, since the flux level at $10\,\mu$m is very low compared to that at $20\,\mu$m. We model this change in flux level by replacing the amorphous silicate dust in the inner disk with dust with a higher continuum opacity. Here we use carbon, but other dust species such as metallic iron may give the same result. This treatment is consistent with that of van Boekel et al. (2004) who found that grain growth in the innermost regions proceeded further than in the outer disk regions. We have not attempted to fit the polycyclic aromatic hydrocarbon (PAH) features in detail, though we implement them into our model to fit the SED. Scattered light contribution is also included and the fraction of the scattered light to the total flux density in 18.8 and $24.5\,\mu$m is 22%–26% in this model.

4.3. The Best-fit Model

We fit the SED as well as the 18.8 and $24.5\,\mu$m images simultaneously by using the disk parameters shown in Table 2. The RBPs and SED of our final best-fit model are shown by the purple dashed lines in Figures 2 and 3. A schematic sketch is given in Figure 4. In this section we will first discuss the geometrical characteristics of the location of the gap and the outer disk properties. Thereafter, we discuss the constraints we find to the inner disk structure of the best-fitting model.

4.3.1. Fitting the SED

Previous SED modeling by Meeus et al. (2010) and Grady et al. (2007) suggested a gap in the disk with an outer radius of 20 and 44 AU, respectively. We confirm and improve on this result by our test modeling for HD 169142: disks without a gap fail to fit the SED, despite various attempts within the physically reasonably parameter space. So already the SED fitting gives a strong indication for the presence of a gap (confirming the results by Meeus et al. 2010; Grady et al. 2007, even though its size is not at all well constrained from the SED alone. We incorporate this result and include a gap in our model. The effect of the discontinuity in the radial density structure is that a large fraction of the stellar light now falls on the vertical
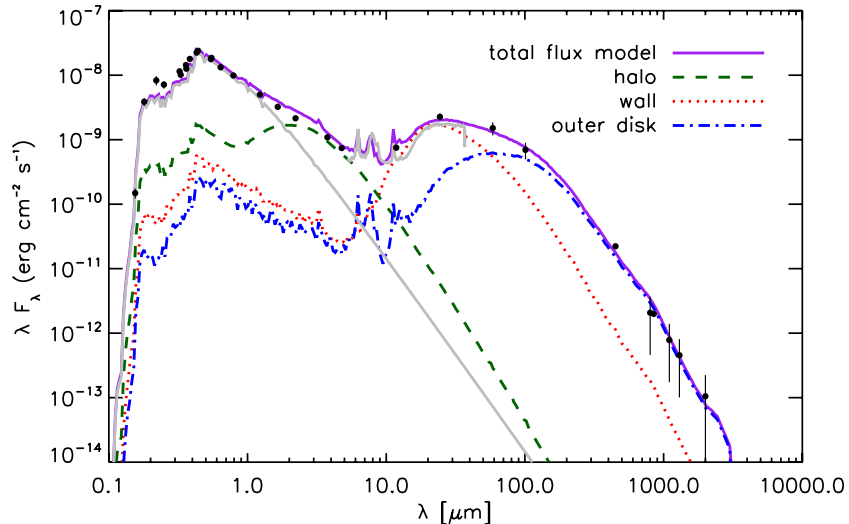
Figure 3. Spectral energy distribution of HD 169142. The solid gray lines represent the Kurucz and *Spitzer*/IRS [5.3–37 μm] spectra, respectively. The dark green dashed line shows the geometrically thick, optically thin halo-like dust cloud component. The red dotted line gives the flux contribution from the innermost part of the outer disk (23–26 AU). The flux from the remainder of the outer disk (26–237 AU) is given by the dot-dashed blue line. The sum of the components is given by the purple solid line. It is clear that at both 18.8 and 24.5 μm, the SED is dominated by flux coming from the inner edge of the outer disk.
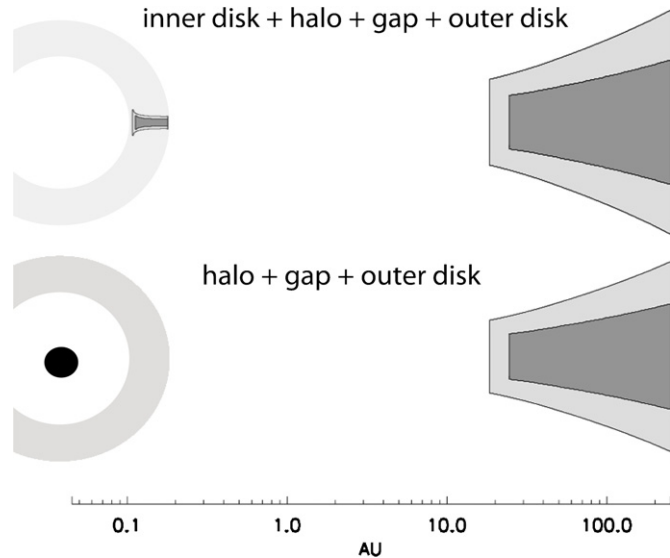

Figure 4. Sketch of our final model with two possible structures for the inner regions. Top: the model with a flat inner disk, an optically thin halo, and an outer disk. Bottom: the model with a denser but still optically thin halo, and an outer disk in which the scale height of the dust is decreased. Both geometries give an equally good fit to the SED and the images. Although we cannot distinguish between these models with our data set, we choose the bottom model as our final model described in the text.

wall at the inner edge of the outer disk. Emission from this wall is clearly distinguishable in the SED (Figure 3, illustrated by the red dotted line). In addition, Figure 3 shows that the flux contribution from the inner edge (between 23 and 26 AU) dominates at 18.8 and 24.5 μm and that flux contributions from the inner regions and from the outer disk are negligible at these wavelengths. Therefore, our Subaru/COMICS images at 18.8 and 24.5 μm are sensitive tracers of the radius where the outer disk starts. Another insight to help understand the dominance of the wall is given by the radial density and temperature plots of the outer disk of this model in Figure 5. The dotted lines show that the densest regions are largely optically thick. Therefore, the temperature of the disk mid-plane decreases rapidly as a function of radius. Thus 18.8 and 24.5 μm photons

are mostly produced at the inner few AU radii of the outer disk.

The radius where the outer disk starts is not well constrained by SED modeling, as the disk structure is degenerate by uncertainties of many parameters, such as the stellar temperature and luminosity, the interstellar extinction, the grain size population of the dust, the vertical density structure, and so on. Only by fitting our model to the resolved MIR observations can we unambiguously confirm the existence of a gap and constrain the location of the wall of the outer disk.

4.3.2. Fitting the MIR Images, Constraining the Location of the Wall

After convolving our best-fit model with the PSFs of the calibrators, we find that the imaging data are best fitted with an inner edge of the outer disk of 23^{+3}_{-5} AU (see Figure 2). The uncertainty on this radius is determined by fitting the uncertainty of the azimuthally averaged flux level at $\pm 1\sigma$. This result is consistent with a wall radius of 20 AU (Meeus et al. 2010) but excludes the model with a wall at 44 AU (Grady et al. 2007).

We have performed a small parameter study where we have examined the robustness of our final model to fit the RBPs at MIR wavelengths. We have varied the following parameters: the surface density power law between $\{-0.5, -1.5\}$, the grain size distribution power law $\{-2.5, -4.5\}$, the dust settling factor $\{0.5, 1\}$, the stellar temperature $\{8000\ \text{K}, 8500\ \text{K}\}$ and luminosity $\{13\ L_\odot, 17\ L_\odot\}$, and the distance $\{130\ \text{pc}, 160\ \text{pc}\}$. While the RBPs vary only slightly in this parameter study (all within the 1σ error of the measurements), the SED fit becomes significantly worse. We conclude that the radius of the wall is the only free parameter which significantly influences the broadness of the RBP. Therefore, our fit to the RBP is robust in constraining the radius of the inner edge of the outer disk at 23^{+3}_{-5} AU.

4.3.3. The Inner Disk

In this section we explain in more detail the implications for the inner disk structure. Modeling shows that an optically thick hydrostatic inner disk does not produce enough flux to fit the SED. Scaling up the vertical height of the inner disk would not be a solution because if the inner disk is higher
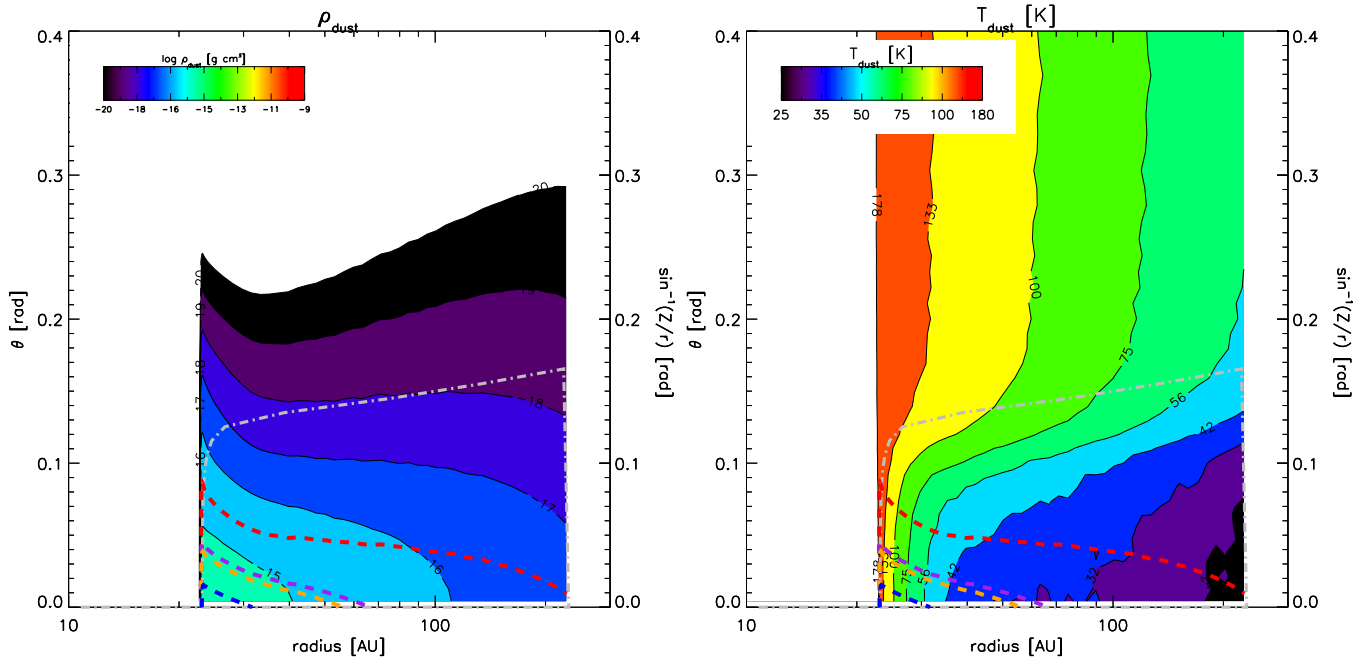
Figure 5. Left: the dust density ρ_{dust} in g cm^{-3} of the outer disk as a function of radius and angle θ for our best-fitting model. The lower and upper density cutoffs are 10^{-20} and 10^{-9} g cm^{-3}, respectively. Right: the temperature structure of the outer disk as a function of radius and angle θ for our best-fitting model. The inner edge of the outer disk starts at a temperature of 180 K. For small θ the angle is approximately Z/r. The gray dot-dashed line shows the $\tau = 1$ surface in radial direction in scattered light ($\lambda = 0.5\,\mu m$). The dashed lines represent the $\tau = 1$ surfaces as seen perpendicular from the disk. From top to bottom the colors are red, purple, orange, and blue and represent the wavelengths 0.5, 18.8, 24.5, and 70 μm.

than $Z/r \sim 0.1$ it covers the outer disk for more than ~50% in direct and scattered light. This inner disk then casts too large a shadow on the outer disk to be able to reproduce the SED at wavelengths longer than ~10 μm. To solve this problem we include a geometrically thick, *optically thin* halo-like dust cloud in the inner regions (<0.5 AU, see Figure 5) to fit the SED in the NIR and to avoid a shadowing effect on the outer disk. The physical origin is not certain at this moment, though other observational studies show that an optically thin component close to the star provides a good fit as well (Grady et al. 2007; Benisty et al. 2011; Verhoeff et al. 2011; Mulders et al. 2010). Furthermore, fitting the Herbig stars' median SED also requires such a halo (Mulders & Dominik 2012). Further high spatial resolution observations such as infrared interferometry will be necessary to reveal the inner disk structure.

If there is no shadowing effect from the inner disk, the wall of the outer disk is too luminous. To fit the SED again, we can either settle the grains in the outer disk by scaling down the dust-density scale height by a factor of 0.6 or we can scale down the abundance of small (<1 μm) grains by one order of magnitude. These adjustments are consistent with dust settling and grain growth (Dullemond & Dominik 2005); however, it is uncertain to what extent these effects are present in the disk. The influence of other effects, like dynamical scattering of larger dust grains may also play a role in the vertical grain size distribution. Alternatively, we can *combine* a halo-like dust cloud and a flat inner disk and consequently perform no settling or removal of small dust grains. So we conclude that there are two possible inner disk geometries (as illustrated in the schematic in Figure 4) which give an equally good fit to the SED and the RBP.

Without an optically thick inner disk, the RBP is still reproduced with the inner radius of the outer disk at 23^{+3}_{-5} AU. The final model can be interpreted as an inner halo-like dust cloud (Krijt & Dominik 2011) and a gas-rich outer disk structure, and so is truly a transitional disk.

5. DISCUSSION

5.1. Is the Inner Hole/Gap Structure Common for Meeus's Group I Sources?

We have shown observational evidence for the presence of an inner hole or gap in the HD 169142 disk. A similar structure is also indicated for other Herbig Ae/Be stars such as AB Aur (Honda et al. 2010), HD 142527 (Fukagawa et al. 2006; Fujiwara et al. 2006; Verhoeff et al. 2011), HD 135344 (Brown et al. 2009), HD 36112 (Isella et al. 2010), and HD 100546 (Bouwman et al. 2003; Benisty et al. 2010; Mulders et al. 2011). All of these objects have been classified as group I according to the definition introduced by Meeus et al. (2001). Since the strong far-infrared excess is a characteristic of group I sources, we speculate that this component may come from the emission from the inner edge of the outer disk. Consequently, we suggest that the inner hole or gap structure may be common for group I sources. If this is true, the hypothesis that group I flared disks evolve into group II flat disks due to dust sedimentation should be reconsidered, because the difference between groups I and II is not only the degree of disk flaring or grain growth, but also the presence of cleared inner regions (holes and gaps) in the disk.

As we have shown in the above analysis, the spatial extent of a Herbig Ae/Be disk at MIR wavelengths, often described by an FWHM, is strongly influenced by the position and temperature of the wall. Previous studies showed that group I sources are likely to be more extended than group II sources in the MIR wavelengths, and suggested that the disk geometry (flaring or flat disk) may play an important role in the thermal structure and MIR emission of the disk (Leinert et al. 2004; Liu et al. 2007; Mariñas et al. 2011). Our 24.5 μm imaging survey of Herbig Ae/Be stars with Subaru/COMICS (M. Honda et al. 2012, in preparation) also confirms that many group I sources are extended. However, their spatial extent shows great diversity, from marginally to remarkably extended. Such diversity in the

spatial extent in the MIR can be understood in terms of the distance, the inner disk structure, and the location of the wall of the outer disk. In fact, the temperature of the wall both in the AB Aur and HD 142527 systems appears to be relatively cool (70–100 K) and its wall radius also tends to be at some distance away from the central star (100 AU in AB Aur; 170 AU in HD 142527; Fujiwara et al. 2006). The wall in HD 169142 is at a smaller distance (23 AU), thus the spatial extent is not so large compared to that of AB Aur and HD 142527. We suggest that not only the geometry (flared or flat) of the disk, but also the inner gap and the wall-like inner edge of the outer disk are important for understanding the spatial extent of Herbig Ae/Be disks in the MIR.

5.2. Origin of the Inner Hole of the HD 169142 Disk

Gaps seem to be a common characteristic of group I flaring disks (Honda et al. 2010; Fukagawa et al. 2006; Fujiwara et al. 2006; Verhoeff et al. 2011; Brown et al. 2009; Isella et al. 2010; Bouwman et al. 2003; Benisty et al. 2010; Mulders et al. 2011). An inner hole or gap in the disk has been explained by several mechanisms, including (1) photoevaporation of the disk (Alexander et al. 2006), (2) geometric shadowing (Dullemond & Dominik 2004), (3) grain growth in the inner disk causing a lower dust opacity zone (van Boekel et al. 2005), and (4) the presence of another body in the disk that dynamically creates a gap and decouples the inner disk from the outer disk (Augereau & Papaloizou 2004). We prefer solution (4) since this also provides a natural explanation for an inner halo-like dust cloud in the inner disk. The presence of a halo likely requires some dynamical interactions with planetary bodies since new generations of dust can then be created in situ up to large disk heights (Krijt & Dominik 2011). Grain growth cannot explain the presence of a gap and a wall. Furthermore, our test models show that geometric shadowing (i.e., varying scale heights, surface density power laws) of a part of the disk at several AU cannot reproduce the SED and the RBP of the images. We recognize that planetary companions have not yet been detected in the transitional disk around HD 169142, though recent direct detection of the planets around A-type stars (e.g., HR8799; Marois et al. 2008, βPic; Lagrange et al. 2010) lends support to such a hypothesis. Thus we suggest that the HD 169142 system is an excellent candidate to look for newly formed planets in the protoplanetary disk.

6. CONCLUSIONS

We arrive at the following conclusions.

1. HD 169142 is extended at MIR wavelengths with the Subaru/COMICS instrument. The derived source sizes from quadratic PSF reference subtraction are $0''.349 \pm 0''.014$ at $18.8\,\mu$m and $0''.261 \pm 0''.025$ at $24.5\,\mu$m, respectively.

2. The observed sizes as well as the steep rise of the SED near $20\,\mu$m require a disk model with an inner hole the size of 23^{+3}_{-5} AU, making HD 169142 a transitional disk.

3. HD 169142 is one of the growing number of Herbig Ae disks that are classified as group I sources and that *also* require the presence of a large inner gap. It appears that many, if not all, group I sources may be strong candidates for classification as transitional disks.

REFERENCES

Acke, B., Min, M., van den Ancker, M. E., et al. 2009, A&A, 502, L17
Alexander, R. D., Clarke, C. J., & Pringle, J. E. 2006, MNRAS, 369, 229
Augereau, J. C., & Papaloizou, J. C. B. 2004, A&A, 414, 1153
Benisty, M., Renard, S., Natta, A., et al. 2011, A&A, 531, A84
Benisty, M., Tatulli, E., Ménard, F., & Swain, M. R. 2010, A&A, 511, A75
Bouwman, J., de Koter, A., Dominik, C., & Waters, L. B. F. M. 2003, A&A, 401, 577
Brown, J. M., Blake, G. A., Qi, C., et al. 2009, ApJ, 704, 496
Cutri, R. M., Skrutskie, M. F., van Dyk, S., et al. 2003, VizieR Online Data Catalog, 2246, 0
Dent, W. R. F., Greaves, J. S., & Coulson, I. M. 2005, MNRAS, 359, 663
de Zeeuw, P. T., Hoogerwerf, R., de Bruijne, J. H. J., Brown, A. G. A., & Blaauw, A. 1999, AJ, 117, 354
Dullemond, C. P., & Dominik, C. 2004, A&A, 417, 159
Dullemond, C. P., & Dominik, C. 2005, A&A, 434, 971
Dullemond, C. P., Henning, T., Visser, R., et al. 2007, A&A, 473, 457
Dunkin, S. K., Barlow, M. J., & Ryan, S. G. 1997, MNRAS, 286, 604
Engelke, C. W., Price, S. D., & Kraemer, K. E. 2006, AJ, 132, 1445
Fujiwara, H., Honda, M., Kataza, H., et al. 2006, ApJ, 644, L133
Fukagawa, M., Tamura, M., Itoh, Y., et al. 2006, ApJ, 636, L153
Grady, C. A., Schneider, G., Hamaguchi, K., et al. 2007, ApJ, 665, 1391
Hellyer, B. 1970, MNRAS, 148, 383
Honda, M., Inoue, A. K., Okamoto, Y. K., et al. 2010, ApJ, 718, L199
Isella, A., Carpenter, J. M., & Sargent, A. I. 2009, ApJ, 701, 260
Isella, A., Natta, A., Wilner, D., Carpenter, J. M., & Testi, L. 2010, ApJ, 725, 1735
Juhász, A., Bouwman, J., Henning, Th., et al. 2010, ApJ, 721, 431
Kataza, H., Okamoto, Y., Takubo, S., et al. 2000, Proc. SPIE, 4008, 1144
Krijt, S., & Dominik, C. 2011, A&A, 531, A80
Lagrange, A.-M., Bonnefoy, M., Chauvin, G., et al. 2010, Science, 329, 57
Leinert, C., van Boekel, R., Waters, L. B. F. M., et al. 2004, A&A, 423, 537
Liu, W. M., Hinz, P. M., Meyer, M. R., et al. 2007, ApJ, 658, 1164
Mariñas, N., Telesco, C. M., Fisher, R. S., & Packham, C. 2011, ApJ, 737, 57
Marois, C., Macintosh, B., Barman, T., et al. 2008, Science, 322, 1348
Mathis, J. S., Rumpl, W., & Nordsieck, K. H. 1977, ApJ, 217, 425
Meeus, G., Pinte, C., Woitke, P., et al. 2010, A&A, 518, L124
Meeus, G., Waters, L. B. F. M., Bouwman, J., et al. 2001, A&A, 365, 476
Meijer, J. 2007, PhD thesis, Astronomical Institute "Anton Pannekoek", University of Amsterdam
Min, M., Dullemond, C. P., Dominik, C., de Koter, A., & Hovenier, J. W. 2009, A&A, 497, 155
Min, M., Hovenier, J. W., & de Koter, A. 2005, A&A, 432, 909
Mulders, G. D., & Dominik, C. 2012, A&A, 539, A9
Mulders, G. D., Dominik, C., & Min, M. 2010, A&A, 512, A11
Mulders, G. D., Waters, L. B. F. M., Dominik, C., et al. 2011, A&A, 531, A93
Okamoto, Y. K., Kataza, H., Yamashita, T., et al. 2003, Proc. SPIE, 4841, 169
Panić, O., Hogerheijde, M. R., Wilner, D., & Qi, C. 2008, A&A, 491, 219
Piétu, V., Dutrey, A., Guilloteau, S., Chapillon, E., & Pety, J. 2006, A&A, 460, L43
Pinte, C., Harries, T. J., Min, M., et al. 2009, A&A, 498, 967
Raman, A., Lisanti, M., Wilner, D. J., Qi, C., & Hogerheijde, M. 2006, AJ, 131, 2290
Sako, S., Okamoto, Y. K., Kataza, H., et al. 2003, PASP, 115, 1407
Sylvester, R. J., Skinner, C. J., Barlow, M. J., & Mannings, V. 1996, MNRAS, 279, 915
van Boekel, R., Min, M., Leinert, C., et al. 2004, Nature, 432, 479
van Boekel, R., Min, M., Waters, L. B. F. M., et al. 2005, A&A, 437, 189
van den Ancker, M. 1999, PhD thesis, Astronomical Institute "Anton Pannekoek", University of Amsterdam
van den Ancker, M. E., The, P. S., Tjin A Djie, H. R. E., et al. 1997, A&A, 324, L33
Verhoeff, A. P., Min, M., Pantin, E., et al. 2011, A&A, 528, A91
Zacharias, N., Urban, S. E., Zacharias, M. I., et al. 2004, AJ, 127, 3043
Zubko, V. G., Mennella, V., Colangeli, L., & Bussoletti, E. 1996, MNRAS, 282, 1321